



Urban gardens in Antiquity The case of Gerasa/Jerash in Jordan

Genevieve Holdridge^{a,b}, Ian Simpson^c, Achim Lichtenberger^d, Rubina Raja^{a,e},
Tim C. Kinnaird^f, David Sanderson^g, Søren M. Kristiansen^{a,b,*}

^a Centre for Urban Network Evolutions (UrbNet), Aarhus University, Moesgaard Allé 20, 8270 Højbjerg, Højbjerg, Denmark

^b Department of Geoscience, Aarhus University, Høegh-Guldbergs Gade 2, 8000 Aarhus C, Denmark

^c Department of Archaeology, Durham University, South Road, Durham DH1 3LE, United Kingdom

^d Institute for Classical Archaeology and Christian Archaeology/Archaeological Museum, Münster University, Domplatz 20-22, 48143 Münster, Germany

^e Department of Classical Studies, School of Culture and Society, Aarhus University, Jens Chr. Skous Vej 7, 8000 Aarhus C, Denmark

^f School of Earth and Environmental Sciences, University of St Andrews, St Andrews, KY16 9TS Scotland, United Kingdom

^g SUERC, University of Glasgow, East Kilbride G75 0QF, Scotland, United Kingdom

ARTICLE INFO

Keywords:

Human impact
Micromorphology
Prehistoric land-use
Urban soil
Roman and early Islamic gardens

ABSTRACT

In the Eastern Mediterranean, where some of the earliest known urban cities are located, relatively little is known about urban soils in archaeological contexts. Red Mediterranean Soil (RMS) is a hallmark of the Mediterranean region while the impact of long-term urbanization on RMS material is understudied. In this article we present evidence of RMS from the longue durée cityscape of Jerash, Jordan, to determine how humans have used, modified and impacted RMS material in an urban context. Thin-sections were made of twelve RMS samples, and micromorphological studies on several in-situ but disturbed soils adjacent to bedrock were conducted, spanning the initial surface soil disturbances in the Hellenistic and Roman period occupation, as well as transported RMS material spanning the Roman through Umayyad periods (until the earthquake of 749 CE). We compared the on-site inner-urban red soils to natural RMS in the area and found that some characteristics reflect their origin in the Pleistocene soils, while other traits reflect human impact related to urban activities. The majority of the on-site samples contained evidence comparable to modern centers, including changes of structure, texture, inclusions, as well as high levels of contamination of heavy metals and phosphorus (P), which combined are strong signs of urban activity. Evidence including textural pedofeatures, fragmented peds, mixed fabrics, sorting of silt-sized material likely reflect the use of RMS in urban gardens and cultivation. Black carbon inclusions within the fabric contain evidence for burning of organic matter in connection with various anthropogenic activities, likely re-dispersed via aeolian and water erosion processes. Heavy metal enrichments, which are associated with production and artisanal activities, may also have been disseminated by both aeolian and surface water processes, possibly in conjunction with irrigation undertaken with polluted water. Contrasting soil fabrics and inclusion features observed in thin section together with elemental analyses characterizes the nature of urban cultivation in its environmental context at Jerash, where city life was maintained for over 800 years. With cultivated soils in urban areas increasingly evidenced in archaeological stratigraphies from different regions of the world, our approach offers new insight into the vital contributions that these soils and their management has made to the food security, resilience and longevity of early city life.

1. Introduction

The study of modern urban soils has come to the forefront in recent time coinciding with the rise of urban population globally and a growing desire for higher urban food security and sustainability (McDougall

et al., 2019). Urban soils are diverse and differentiated by parent materials, anthropogenic activities including industry, construction, and agriculture/gardening, impact intensity and age (Pereira et al., 2016). Human disturbances such as mixing, moving, compaction, and additions of urban artifacts including industrial waste, organic compost,

* Corresponding author at: Centre for Urban Network Evolutions (UrbNet), Aarhus University, Moesgaard Allé 20, 8270 Højbjerg, Højbjerg, Denmark.
E-mail address: smk@geo.au.dk (S.M. Kristiansen).

<https://doi.org/10.1016/j.jasrep.2022.103633>

Received 6 April 2022; Received in revised form 28 July 2022; Accepted 1 September 2022

Available online 7 October 2022

2352-409X/© 2022 The Authors. Published by Elsevier Ltd. This is an open access article under the CC BY license (<http://creativecommons.org/licenses/by/4.0/>).

household garbage and building materials may result in negative and/or positive effects on soil structure, fabric and fertility (e.g. Amossé et al., 2015; Lehmann and Stahr, 2007). Urban soils generally have higher bulk density, lower microbial biomass and activity, higher nitrification rates, higher pH, lower CEC, an external or ex-situ component, and in some cases enhanced development as compared to natural and less impacted soil systems (Pereira et al., 2016; Amossé et al., 2015; Yang and Zhang, 2015; Scharenbroch et al., 2005). One of the main characteristics of modern urban soils is contamination or pollution with heavy metals, in particular, Cu, Pb, and Zn, and organic pollutants including polycyclic aromatic hydrocarbons, which accumulates in urban soils, as well as in soils and sediments in city hinterlands (Horváth et al., 2016; Lehmann and Stahr, 2007; Pereira et al., 2016; Yang and Zhang, 2015).

Studies of past urban environments have shown that urban soils have a long history of disturbance and modification by human activities but have often been disregarded as dump or waste. However, for example the so-called ‘anthropogenic dark earths (ADE)’ of the late Roman and Medieval periods in Europe (Devos et al., 2017; Macphail and Goldberg, 2017; Nicosia et al., 2012; Kristiansen, 2018; Wouters et al., 2017), in Pre-Columbian Amazonia (Schmidt et al., 2014) and contemporary Sub-Saharan Africa (Solomon et al., 2016) reflect mixed uses of urban spaces such as middens, markets, domestic areas, and gardening. The use of ADE involves fertilizing smaller patches of local soils with large amounts of anthropogenic organic and burnt organic waste, biochar, and sometimes building debris, likely together with a high input of water and labor per area to achieve high yields of protein rich soil (Solomon et al., 2016).

In the Eastern Mediterranean, where some of the earliest known urban cities are located, relatively little is known about urban soils in archaeological contexts. The soil catena of the Mediterranean region is highly diverse (Martin-Garcia et al., 2004; Sandler et al., 2015; Yaalon, 1997), though many of these soils display a characteristic red color (5YR to 10R Munsell hues), and are referred to as ‘Red Mediterranean Soil(s)’ (RMS) (e.g., Fedoroff and Courty, 2013; Yaalon, 1997). ‘Red Mediterranean Soil’ is a term that has been used to refer to soils forming under Mediterranean climatic conditions globally (e.g. xeric conditions; see Fedoroff and Courty, 2013 for summary on paleoclimate) and associated with well-lithified limestone or dolostone (Vingiani et al., 2018; Yaalon, 1997; Fedoroff and Courty, 2013; Lucke et al., 2014a, 2014b; Sandler et al., 2015). Although some studies have shown human impact on the texture, structure and content of RMS in landscape studies (Priori et al., 2008; Schmidt et al., 2006), there is little information on whether RMS and/or RMS material have had a special use in ancient urban contexts and environments. Furthermore, post 12th century Arabic manuals of agriculture, gardening and manuring practices from Syria and Yemen have been somewhat neglected in Anglophone literature; an introduction and references to relevant works can be found at *The Filaha Texts Project* (<https://www.filaha.org/>).

Today, gardening or horticulture is considered as cultivation *per se* but as distinctly different from agriculture because they are smaller plots that are used for mixed, well-managed crops, including fruit trees. Crop diversity, high food security and distinctive social structures that underpin gardens they have actually never been identified and disentangled from large-scale agriculture, and recently, Bogaard (2005) discussed “garden agriculture” as a possible separate trait of human ecology. Although the definition of gardening, horticulture and intensive cultivation of smaller plots in an sedentary archaeological context is often unclear and encompasses a variety of different cultivation methods and management systems (Price and Bar-Yosef, 2011), archaeological evidence of small-scale intensive land-use exists from a variety of areas and sources including Mediterranean archaeological urban sites, such as from the Greek Island of Evvia (Jones, 2005), and from Cato the Elder’s (234–149 BCE) general descriptions of Roman non-ornamental gardens. According to other historical Roman texts, gardens received mixed materials including fertilizers from human and animal manure, kitchen waste, as well as green manure from certain plants (Farrar (1998);

Columella 1941: 196–201). Gardens studied by Delgado et al., (2007) and Wilkinson (1988) from the Classical and Medieval periods in the Mediterranean and Near East contained urban refuse, such as diverse types of organic waste, building materials, industrial waste and occupational debris, though this is rarely discussed as intentional but merely seen as a by-product of the long-term human occupation around them. Jashemski (2016) found in an overview of existing archaeological information on Roman produce that kitchen gardens were an important source for fruits and vegetables as these were an essential part of Mediterranean diet in Antiquity as they are today. Archaeological evidence of kitchen gardens is also present in drier climate-zones like present-day eastern Egypt. Evidence for elaborate care in bringing in good soil to gardens were found, but no specific properties of such soil material was mentioned for sites from drier climates.

Studies of on-site geochemical analyses from archaeological contexts indicating heavy metal and/or organic substance contamination or pollution are sparse, especially in relation to RMS in the Eastern Mediterranean region. However, a few studies have discerned increased concentrations of heavy metals in soils of several Bronze Age settlement (Šmejda et al., 2018; Homsher et al., 2016), and in a Roman garden in Jordan (Bedal et al., 2013).

In summary, the human impact on and use of RMS is an overlooked topic in the Eastern Mediterranean region, despite the fact that such studies may offer valuable insights into past human activities and may improve the understanding of natural soil genesis.

In this paper we examine anthropogenic impact on RMS at the ancient city of Jerash located in northern modern Jordan. This site was continuously occupied from the Hellenistic period through the Umayyad period (i.e., 2nd Century BCE to mid-8th Century CE), and after a period of drastically reduced population, it was later resettled during the middle Islamic period (13th/14th century CE) until the present (Lichtenberger and Raja, 2015, 2018b; Lichtenberger and Raja, 2018a; Lichtenberger and Raja, 2019). Our specific aims are: 1) to characterize the RMS material on and around the archaeological site of Jerash, 2) comparing to it to adjacent non-RMS material in the area, and Jordan and in the Mediterranean in general; and 3) to determine how humans have used, modified and/or impacted RMS soil material in an urban context.

2. Materials and methods

2.1. Study location

The focus of the investigations is the Northwest Quarter (NWQ) of the urban site (part of the Danish-German Jerash Northwest Quarter Project, Lichtenberger and Raja, 2015) of ancient Jerash (Fig. 1). The city was re-founded in the 2nd century BCE in the wake of Alexander the Great’s conquest of the East and thrived throughout the Hellenistic and Roman periods (Raja, 2012). In the Late Roman, Byzantine and Early Islamic periods, the city continued to expand and only a devastating earthquake in AD 749 brought an end to urban life in the site Philippsen and Olsen (2020). Today, the site is the second most visited archaeological site in Jordan, due to its good preservation and monumental Roman period ruins, only surpassed by Petra. Jerash (coordinates: 32°16′43.46″N and 35°53′28.67″W) is located in semi-arid climate zone (BSh) of the Jerash province in the Ajloun highlands (Köppen Classification, Boyer, 2018). The Ajloun highlands are situated in northwest Jordan, and comprise steep relief and varying geology including limestones, sandstones, shales with Triassic, Jurassic, and Cretaceous ages, as well as Quaternary alluvium (Bender, 1974). The geologic formations observed at the archaeological site are summarized by Holdridge (2020) and limestone and conglomerate formations dominate. Shrubland or maquis comprises the majority of vegetation in Jordan on limestone, especially in altitudes above 700 m (Al-Eisawi, 1985). No hematite rich geological strata are known from the area. During the NWQ excavation campaign >100 m of profiles has been exposed while only a few

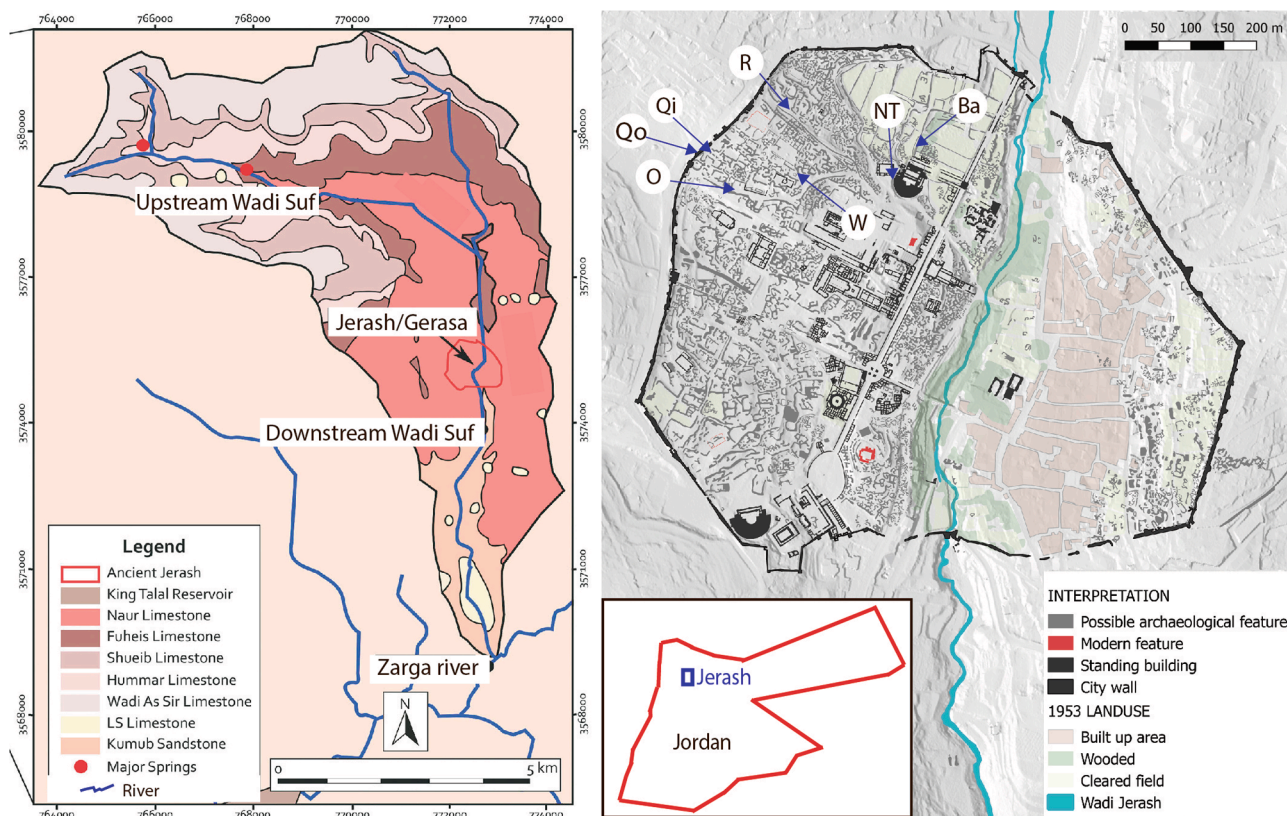


Fig. 1. Map of Jerash's location in Jordan, and an overview of sampled archaeological trenches within Jerash, and the hinterland in Wadi Suf. Sampled trenches from within the ancient city are denoted as follows: Basilica (Ba), North Trench (NT), Trench O (O), Trench R (R) and Trench W (W). Trenches respectively within and without the city wall are denoted Q inner (Qi) and Q outer (Qo). Background maps with the ancient settlement layout is modified from [Stott et al. \(2018\)](#) and the regional geology from [Holdridge \(2020\)](#).

fragments of RMS was identified (discussed below) suggesting very intensive disturbance of the pre-urban soil surface. The geomorphology of the wadi is discussed in [Holdridge \(submitted\)](#). Full context ID, stratigraphic correlations and samples ID in relation to the context numbers are shown in Appendix A, [Supplementary Material](#), Tables S1.1 to S1.7.

2.2. Natural soil formation in the region

The soils in the province of Jerash reflect the expected diversity of RMS, and their relationship to topography, geology and climate ([Lucke et al., 2013](#)). Red Mediterranean Soils in the Jerash area include mainly Cambisols and Vertisols (with Vertic, Calcic, Chromic, Luvic Haplic, and Cambic horizons), which are prevalent throughout the subhumid to semiarid climate regimes of the Ajloun highland region ([WRB, 2015](#); [Lucke et al., 2013](#); [Al-Qudah, 2001](#)). Much of the RMS in the region are formed on limestone, although some have been found on sandstone and basalt, and they are more developed on flatter areas ([Lucke et al., 2014a, 2014b](#); [Lucke et al., 2013](#)). Yellow Mediterranean Soil(s) (YMS), referred to as Cambisols or Calcisols, are prevalent in steeper areas in the northwest and surrounding western highland area of Jordan ([WRB, 2015](#); [Lucke et al., 2013](#); [Al-Qudah, 2001](#)). The RMS are the most prominent soil in Mediterranean climates of Jordan and considered to be very fertile, though like other RMS (see [Fedoroff and Courty, 2013](#); [Priori et al., 2008](#)) they typically have low amounts of organic matter/high organic turnover ([Lucke et al., 2014a, 2014b](#)). Other key characteristics of RMS including those in Jordan, involve rubefaction in relation to the formation of hematite, which give them a hue of 2.5YR to 10YR ([Sandler et al., 2015](#)), co-illuviation of clay and Fe oxides, carbonate dissolution and accretion, neutral pH, and a well-drained pedon ([Fedoroff and Courty, 2013](#); [Priori et al., 2008](#); [Sandler et al., 2015](#);

[Yaalon, 1997](#)). In Jordan, low nitrogen, and sometimes low amounts of Fe, Zn and P due to their high calcium carbonate content have also been observed ([Lucke et al., 2013](#); [2014a, 2014b](#)). Geochemical and clay mineral studies from [Lucke et al. \(2013, 2014a, 2014b\)](#) indicate that like other RMS (e.g., [Vingiani et al., 2018](#); [Yaalon, 1997](#); [Fedoroff and Courty, 2013](#); [Sandler et al., 2015](#); [Muhs et al., 2010](#)), the origin of RMS in Jordan is linked to long-time bedrock dissolution as well as aeolian input. Aeolian clay mineral additions such as high amounts of smectite and vermiculite, are important sources for major elemental input. Other clay and fine silt-sized aeolian material additions include mainly quartz (35–45%) and lesser amounts of calcite, dolomite, feldspar, halite, and gypsum ([Lucke et al., 2014a, 2014b](#)). Geochemical and mineralogical studies of RMS throughout the Mediterranean have shown that sources of aeolian material is dust from North Africa ([Vingiani et al., 2018](#)), or the Arabian Desert ([Awadh, 2012](#); [Kalderon-Asael et al., 2009](#)). Similarities in geochemistry and mineralogy support the hypothesis that at least some of the dust sources in Jordan are from the east Sahara including Sudan and Egypt ([Lucke et al., 2014a, 2014b](#)).

Few RMS formations are attributed to metasomatic replacement of limestone and/or dolostone (e.g., [Merino and Banerjee, 2008](#)), including only one observation in Jordan ([Lucke et al., 2012](#)). Like other RMS (e.g., [Fedoroff and Courty, 2013](#); [Durn, 2003](#)), the RMS in Jordan appear to have polygenetic attributes resulting from various climate changes during the Pleistocene, involving high clay content, clay films, and precipitation of hematite developed during past humid conditions ([Lucke et al., 2014a, 2014b](#)). In contrast, aspects of reworking and colluvial additions in RMS are linked to major erosion during the Late Glacial and the Younger Dryas (e.g., [Fedoroff and Courty, 2013](#); in Jordan: [Lucke et al., 2013](#); [Schmidt et al., 2006](#)). Ages of RMS in Jordan suggest that they formed during the Pleistocene ([Lucke et al., 2014a, 2014b](#); [Lichtenberger et al., 2019](#)).

2.3. Existing soil science evidence from Jerash

Previously reported soil parameters include 1) effective cation exchange capacity (ECEC) measurements summarized by Holdridge et al. (2020), 2) optically stimulated luminescence (OSL) quartz ages of some RMS materials examined offsite (Lichtenberger et al., 2019; Holdridge et al., 2021), 3) soil geochemistry of profiles within the ancient city (Holdridge et al., 2021) and 4) off-site and within ancient city particle size and geochemical analyses reported by Holdridge (submitted) and Holdridge et al., (2021), respectively. Evidence here revealed that the on-site red horizons are either intact pedogenic or moved by human endeavor to create a placed red horizon. The related ancient urban water management is discussed by Stott et al. (2018), Lichtenberger and Raja (2020) and Passchier et al. (2021).

2.4. Field sampling and laboratory analyses

Several in-situ and ex-situ red and yellow (Munsell color characterized) soils and soil material were observed in ancient Jerash and the surrounding hinterlands of Wadi Suf. Much of the information concerning the RMS and YMS in the surrounding wadi are field observations, while more detailed geochemical information from RMS in Jordan is found in Lucke (2013).

Intact inner-city RMS was very rare while small fragments or clods of red and yellow materials were found distributed widely in excavated trenches. In 2015–17, soil descriptions were made of four excavated stratigraphic sections in the NWQ (Trenches Q, R, O and W; Fig. 1); twelve undisturbed samples for thin section manufacture and micromorphology together with associated bulk samples were obtained of RMS material that was in-situ (e.g., over bedrock or as part of a pedogenic horizon sequence) and ex-situ (moved and placed to the location from elsewhere and now within a sedimentary horizon sequence). A further two already exposed deep urban profiles namely the Basilica-complex and the North Trench, were cleaned. From these profiles, along with Trench W, 19 stratigraphically controlled samples of non-RMS soils or sediments were collected as well as five RMS soil samples were obtained from the North Trench and Trench W profiles. Descriptions of the soils and sediments were made using the USDA Soil Survey Staff field book (2003) and classified according to WRB (2015).

Thin sections were prepared at the University of Stirling Thin Section Micromorphology Laboratory following standard procedures of acetone replacement of water, resin impregnation and curing, mounting on a glass slide, slicing then lapping to 30 µm thickness (<https://www.thin.stir.ac.uk>). Descriptions of the thin sections were undertaken with an Olympus BX-51 polarising microscope and utilized plane-polarised light (PPL), cross-polarizers (XPL), and oblique incident light (OIL). A range of magnifications (x2 – x40 objectives) were used with standard visual aids employed, with semi-quantitative estimations, descriptive terminology and selected quantitative assessments following Bullock et al. (1985) and Stoops (2003). Slide description protocols involved a first assessment to give a first approximation, a second assessment to test and confirm the first approximation, and a third assessment to consider unusual features. Interpretation of features was aided by Ishawari (2013) for coarse mineral material, Durand et al. (2010) for calcium carbonate features and Adderley et al. (2018) for anthropogenic features.

All of the bulk soil and sediment samples were pre-processed at the Department of Geoscience, Aarhus University. After air-drying, samples were < 2 mm sieved and milled in a Tungsten-Carbide mortar. Sub-samples for total geochemistry analysis by Inductively Coupled Plasma Mass Spectroscopy (ICPMS) was sent to Bureau Veritas Commodities, Vancouver, Canada. Sample pre-treatment included heating in a mixture of HNO₃, HClO₄ and HF, taken to dryness and finally dissolved in HCl, a procedure that dissolves nearly all minerals. The analytical accuracy was evaluated by including standard soil samples with known concentrations. Elements found in sufficiently high concentrations above

detection limits, and with sufficient precision in repeated analyses (Pearson R > 0.9), were (in alphabetical order): Al, Ba, Ca, Ce, Co, Cr, Cs, Cu, Dy, Er, Fe, Ga, Hf, K, La, Li, Mg, Mn, Na, Nd, Ni, P, Pb, Pr, Rb, Sb, Sc, Sm, Sn, Sr, Th, Ti, Tl, U, V, Y, Zn and Zr. Only selected anthropogenic elements (sensu Sulas et al., 2019) are discussed here, the rest is used in the multivariate statistical analysis only to group the samples. Please notice that averages of Cu and Pb previously have been shown in a figure in Holdridge et al. (2020) as “within city” contents.

2.5. Statistics

The soil geochemical data was analyzed with a multivariate statistical analysis prior to interpretation of the overall results. The chemical data was analyzed using both descriptive statistics and Principal Component Analysis (PCA) allowing a better understanding of the multivariate dataset. The PCA procedure and interpretations followed recommendations by Esbensen (2004). As the concentrations of the elements varied over several magnitudes, the data was scaled to mean zero and unit variance. Several PCA models were run on the full as well as different reduced datasets, but the most informative pattern of sample and element distribution was obtained using the full dataset. All calculations and figures were made in Python 3.6 (the Numpy, Pandas, scikit-learn and Matplotlib modules).

3. Results

3.1. Red Mediterranean Soil: Contexts and macromorphology

In the hinterlands of ancient Jerash, RMS material was commonly observed along fluvial terraces adjacent to the wadi in the upper watershed, both in situ (Fig. 2a), buried and disturbed (Fig. 2b,d,e,g). Transported RMS material was observed associated with a small farm and a plant nursery located on a recent artificial terrace along the wadi, just downstream from the site of Jerash (Fig. 2c,f). The observed RMS material ranges in color from red (5YR 4/4) (silty) clay loam to reddish brown (7.5YR 5/4) silty clay loam, while yellow soil material (7.5YR 8/2) is a silty to sandy silty loam. The various soil material has fine to medium subangular blocky structure.

Inside and adjacent to the ancient Roman period city walls RMS was rare but could be collected from a number of trenches in the NWQ (e.g., Trenches Q, R, O, and W). The soil ranges from red (7.5YR 3/4) (silty) clay loam, brownish red (7.5YR 5/4–5/8) silty clay loam and fine sandy silty loam, while the yellowish material consists of (7.5 YR 8/2) silty loam to sandy silty loam. Where peds were relatively intact, the soil structure ranged from weak to moderate, fine subangular blocky, to moderate, medium subangular blocky.

Samples of RMS and YMS material were collected from the bases of Trenches Q and O (Fig. 1, 2b), some of which were relatively intact while others were clearly disturbed. Trench Q traversed a small section of the city wall, allowing for examination of the soils and sediments inside, below and outside the wall. The city wall was constructed in the second century CE (Lichtenberger and Raja, 2019) on top of the more intact RMS fragments. One of the samples came from an RMS inside the city wall overlying bedrock (Trench Q, sample Q Inner Red), while four others were obtained from the same trench directly outside the city wall. Two of these latter samples comprised an A2-Bw sequence of RMS material (samples Q Red Upper, Q Outer Red Lower), while the other two (sample Q Outer Red) belonged to a soil A2-Bw sequence over an YMS (sample Q Outer Yellow). Both sequences overlay bedrock and were intact.

The micromorphological sample from Trench O (sample O24104) was obtained from RMS material near the underlying bedrock situated outside and at the base of the northwestern corner of a large cistern in use from the Roman to Byzantine period (Lichtenberger et al., 2015). The building of residences and use of space around the cistern during these periods appear to have been related to the function of the cistern as



Fig. 2. Image of Red Mediterranean Soil (RMS) within the urban area of Jerash and in the Wadi Suf watershed. 2a) in situ RMS within the ancient city, b) is reworked RMS within the ancient city; 2c) imported RMS material along Wadi Suf for contemporary gardening; 2d), e), g) buried RMS in Wadi Suf (highlighted by dashed red lines); and 2f) use of RMS material for planting in a local plant nursery. (For interpretation of the references to color in this figure legend, the reader is referred to the web version of this article.)

a water supply (Kalaitzoglou et al., 2015).

Trench R is located on the northern slope of the Northwest Quarter. Two of the samples from this trench (R24 Upper and Lower) came from a disturbed RMS near bedrock, which based on archaeological finds suggests a Roman age, while two other samples (R1920 and R9) from Trench R came from soil material that was not associated with bedrock, but was apparently transported from elsewhere (Fig. 3a and b). Sample R9 was obtained from a thin red soil material layer, interpreted in the

field as belonging to a pathway, while sample R1920 was collected from a very mixed archaeological layer. Both of these samples contain evidence of mixed late Roman and early Byzantine occupation. Trench R has been interpreted as an open space, potentially for communal activities (Kalaitzoglou et al., 2015), which contained material dating to the Roman period.

Red Mediterranean Soil material was also obtained from two layers observed in the profile of Trench W, located towards the south slope of

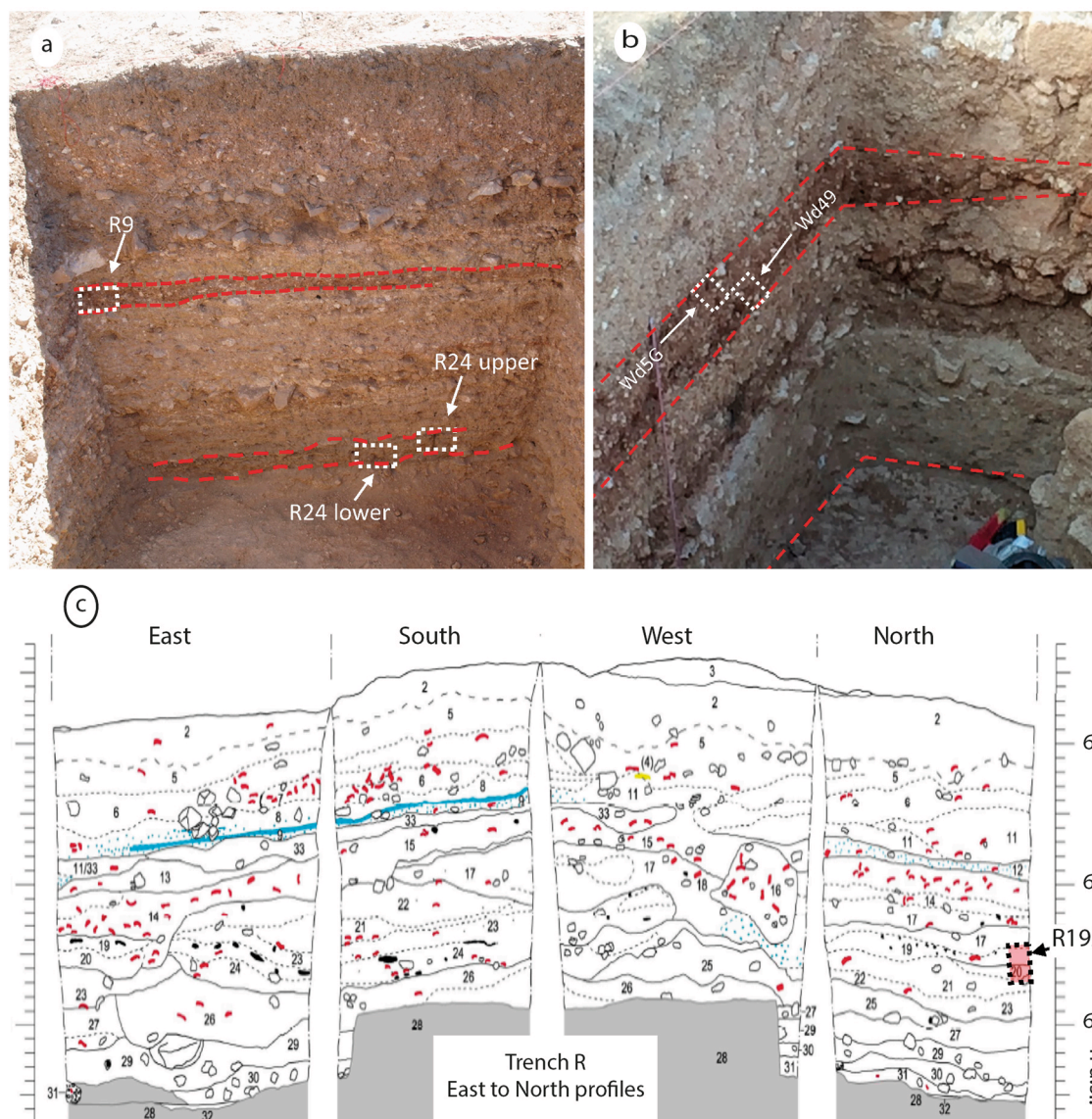


Fig. 3. Red Mediterranean Soil (RMS) and RMS material observed in the Northwest Quarter of Jerash, Jordan. 3a-3b images of RMS material in Trench R and W (highlighted by red dashed lines), the upper is transported RMS soil material, while the lower is a disturbed, buried RMS above bedrock. (For interpretation of the references to color in this figure legend, the reader is referred to the web version of this article.)

the Northwest Quarter, (samples Wd4g, Wd5g) (Fig. 3c). The RMS samples from Trench W corresponded to an open space that was adjacent to and associated with a Byzantine period structure, a mosaic hall with dated inscriptions (Lichtenberger and Raja, 2018b). The upper of these two soil horizons (Wd4g) is more fragmented and less red, while the lower is clay rich and has a darker red color (Wd5g). At the bottom of Trench W, a disturbed RMS was located above bedrock that was associated with Roman material, but no micromorphological sample was taken as it was too thin to sample.

Our WRB soil classification was based on the rule that the overlying material and the buried soil are classified as one soil (WRB, 2015, p. 21), as all our profiles only had fragments of buried surfaces or material with RMS properties (i.e., cambic and terric properties). The profiles R, BN and NT are accordingly classified as Colluvic Regosols, while all profiles in Q, W and O are Urbic Technosols (Appendix A Supplementary data Table S1).

3.2. Micromorphology

Table S1 in Appendix A Supplementary S2 and S3 data gives full and concise and comparative micromorphological descriptions of the thin sections. Additional descriptive information on coarse material fabric arrangement is also given in the text.

3.2.1. Fine material/micromass (<10 μm)

All samples have a complex micromass but which can be resolved to one or more of three types: (1) red to reddish brown, with stipple speckled b-fabric (Fig. 4e and f); (2) reddish-brown with occasional red - yellow - brown, weakly stipple-speckled and calcitic crystallitic b-fabric (Fig. 4c and d); and/or (3) yellow, with calcitic crystallitic b-fabric (Fig. 4a and 4b). For types (1) and (2), clay appears speckled in PPL, while in XPL, weak interference colors are discerned as speckled b-fabric, which is weaker and patchier in type (2). Limpidity is highest in type (1) and least in type (3); localized, areas in the slides containing types (1) and (2) appear yellow brown, which may be organic matter that is also contributing to increased opaqueness. The calcitic crystallitic

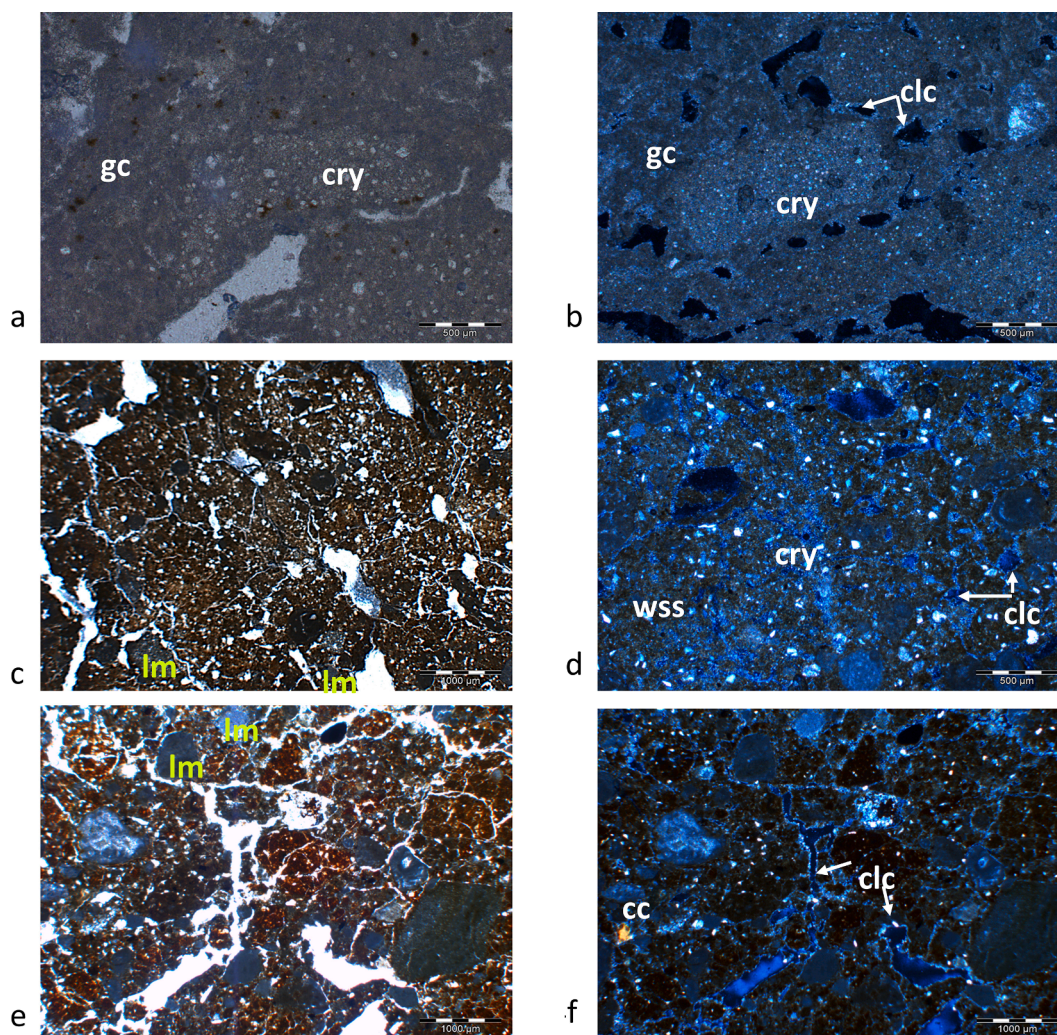


Fig. 4. Micromorphological images 4a) (PPL; 500 µm) and 4b) (XP; 500 µm; both micromass type 3) from Profile Q Outer Yellow including calcitic crystallitic (cry) fabric with grey clay (gc); note calcite coatings (clc) around voids in 4b). 4c) Example of predominantly reddish-brown, speckled fine material (PPL; 1000 µm) and 4d) weakly stipple speckled (wss) and calcitic crystallitic (cry) fabric in Q Outer Red Lower (both micromass type 2; XP; 500 µm). 4e) Example of red, speckled fine material (PPL; 1000 µm) and 4f) weakly stipple speckled fabric (wss) (XP; 1000 µm) in sample R9 (both micromass type 1). Note the few and frequent, subrounded to subangular limestone clasts in Q Outer Red Lower (4c, PPL) and R9 (4e, PPL), respectively. Also note the higher clay content in R9 (4e, PPL), (areas of bright yellow in fabric) and the occasional clay coatings (cc) on grains in R9 (4f, XPL). Calcite coatings (clc) along voids are observable in 4d) Q Outer Red Lower and 4f) R9; (both XPL). Note in slides 4c-4f the distribution of quartz grains, and lack thereof in 4a and b. (PPL - Plane polarized light; XP - Cross polars; scale bar in µm). (For interpretation of the references to color in this figure legend, the reader is referred to the web version of this article.)

b-fabric observed in types (2) and (3) contains small high birefringent grains with moderate to high interference colors in XPL. Type (3) also has areas of grey in PPL, indicating some amorphous clay.

In general, most of the thin sections show a degree of mixed fabrics. In several, including thin-sections of Q Outer Red Upper, Q Outer Red, Q Inner Red, O24104, R24 Upper, Wd49, there is a common frequency micromass type with subordinate (few) micromass type; other thin sections, including Q Outer Red Lower, R1920, R9, R24 Lower, and Wd5g, contain similar frequencies of micromass types (1) and (2). Q Outer Yellow is the only thin section containing type (3); this yellow, calcite crystallitic fabric is associated with the less weathered or weathering limestone parent material. Very few to few areas or patches of this fabric in types (1) and especially (2) suggest that important components of these soils are also weathered or weathering limestone. In some cases, the weathering is relict or incorporated into the soils over longer periods of time, while more localized areas of weathering are associated with clasts of weathered limestone. These observations support the importance of local parent material in the formation of RMS here as in other areas (see also Fedoroff and Courty, 2013; Priori et al.,

2008; Sandler et al., 2015; Yaalon, 1997).

3.2.2. Coarse material (>10 µm)

The coarse material arrangement was random in all samples. Moderate to poor sorting was observed in thin-sections Q Outer Red Upper, R9, and Wd5g, while slides Q Outer Red Lower, Q Inner Red, Q Outer Yellow, R1920, Wd4g, R24 Upper and Lower exhibited poor to very poor sorting. Q Outer Red and O24104 are well sorted in both their silt fraction and coarse quartz fraction. The textures of samples R9, Q Outer Red Lower, Q Inner Red was sandy clay loam, while that of Q Outer Red upper was silty clay loam. Q Outer Yellow comprises a silty loam. The texture of the rest of the thin sections comprised clay loam. In general, the coarse to fine related distribution in all samples was double space to open porphyric with the exception of the chitonic Q Outer Yellow sample.

Eolian or allochthonous coarse mineral contribution was observed in our RMS samples, as in other RMS locations (e.g., Vingiani et al., 2018; Priori et al., 2008; Fedoroff and Courty, 2013; Muhs et al., 2010; Lucke et al., 2014a, 2014b). These additions include few to frequent silt to fine

sand-sized subangular, smooth quartz, and trace amounts of other minerals (mica, feldspar, and glauconite), observed in all samples except for Q Outer Yellow, where there were only trace amounts of quartz grains. Due to the trace amounts and sporadic appearance of these quartz grains in the latter sample, it is suggested that they are incorporated from the overlying layer (O Outer Red W). Counts of quartz grains were on average 58 per grid, and they had an average size of 29 μm . Quartz grains were typically randomly distributed except in Q Outer Red and in particular sample O24104 where there are occasional areas of dense grain clustering and spaces void of grains. Very few sub-rounded, smooth red to yellow mineral oxides (cryptocrystalline) were observed in all samples except Q Outer Yellow, though slightly more red oxides inclusions were observed in Q Inner Red than in other in samples. These are interpreted as being aeolian additions and not formed in situ as pedofeatures (Fig. 5).

There were few, randomly distributed, limestone rock fragment inclusions in samples Q Outer Red Upper and Lower, R24 Lower, and Wd5g, while frequent, to common randomly distributed limestone is evident in slides Q Outer Red, Wd4g, O24104, R24 Upper, R9 and R1920. No lithic limestone was observed in thin-section Q Outer Yellow. The majority of rock inclusions consist of a dark grey limestone, ranging from silt sized grains (56 μm) to granule-sized clasts (2500 μm), with most clasts corresponding to fine and medium sand-sized fragments (average is 358 μm with 157 μm standard deviation). Much of these rock fragments show signs of variable recrystallization formed by secondary carbonate precipitation in pores indicating they are weathered. All limestone clasts have sub-rounded to subangular shape, having been rounded by fluvial transport.

3.2.3. Microstructure and porosity

All sample have channel and chamber micro-structures; samples O24104, R24 Upper and Lower and Wd4g and Wd 5g also have a dominant micro-aggregate structural element. Where channel and

chamber is the microstructural class, weak to strong sub-angular blocky peds predominate; where micro-aggregates are the dominant structural element weak spheroidal crumb is the ped class. Channel and Chamber voids are evident throughout all thin sections with packing void variants in samples Q Outer Red E upper, O24104 and planar voids in samples Q outer yellow Q Outer Red E lower and R9. Total porosity ranges from 6% (Q Inner Red; R1920) to 30% (Q Outer Red Upper; R24 Lower), with the other samples ranging between 10 and 25%.

There is no strong contrast in microstructure, ped and void features between the three micromass fabrics identified, perhaps giving a distinction between features more readily modified by land management (microstructure) and those that are inherently more stable (micromass). With regard to the former we highlight here the occurrence of micro-aggregate structures and fragmented peds within the city wall boundary, features that are absent from our RMS samples from immediately beyond the city wall.

3.2.4. Pedofeatures

The red to reddish brown, speckled b-fabric of type (1) is attributed to peds that were coated to varying degrees with clay and Fe oxides, which is related to their co-illuviation (as in [Fedoroff and Courty, 2013](#); [Priori et al., 2008](#); [Sandler et al., 2015](#); [Yaalon, 1997](#)) (Fig. 4a through 4d). The distribution of clay and Fe oxides in the micromass of RMS is related to clay illuviation, which occurs in present day humid and sub-humid zones on the fringe of the Mediterranean basin, and suggests that in present arid areas, these features may be inherited from earlier, more humid periods ([D'Amico et al., 2016](#); [Fedoroff, 1997](#)). Since it is unclear if the source for clay and Fe oxides derives from local, in-situ processes or results from aeolian input, we link the reddening of the soils to oxidation processes (vs. rubification) and the well-drained topography (as in other RMS, see [D'Amico et al., 2016](#); [Sandler et al., 2015](#); [Fedoroff and Courty, 2013](#)). Well-drained topography, such as the permeable limestone at Jerash, allows for local desiccation, which are

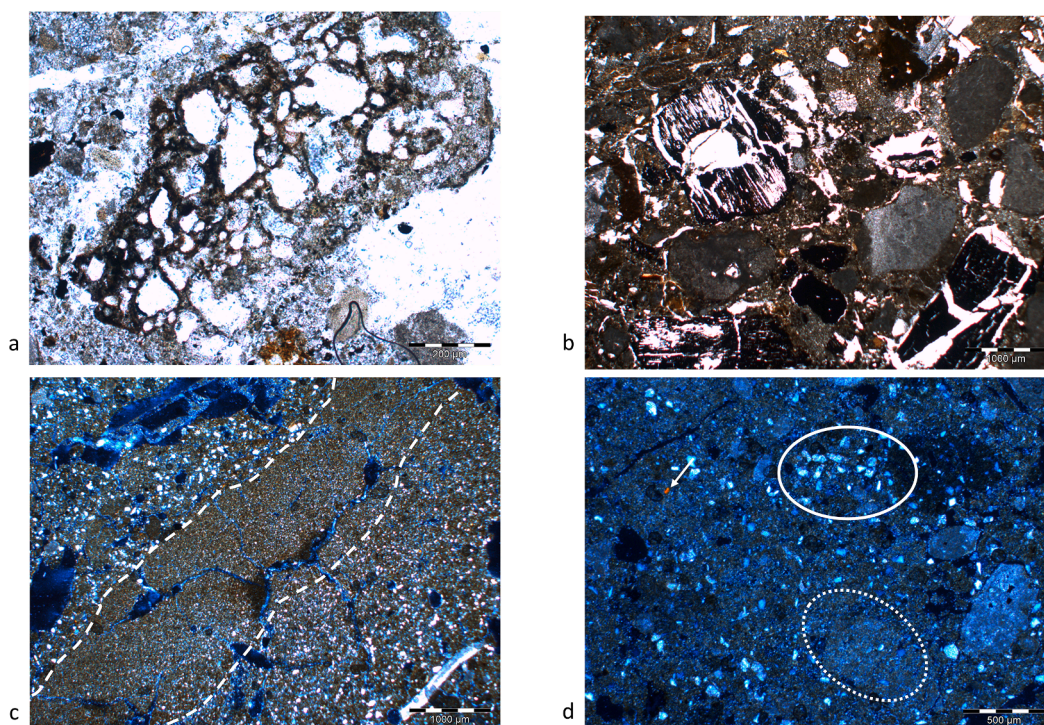


Fig. 5. Micromorphological images 5a) R24 (200 μm ; 5b) R24 (1000 μm). 5c) Well sorted aeolian quartz grains slide O24014 (XPL; 1000 μm), area of quartz grain depletion highlighted by white dashed lines. 5d) (XPL 500 μm); Moderate sorting of aeolian quartz grains (example of clustering highlighted by white solid circle vs. example of area with greatly reduced grains highlighted by white dashed circle) in fabric of Q Outer Red. Note the rounded, likely aeolian-transported, Fe oxide grain (white arrow). (PPL - Plane polarized light; XP - Cross polars; scale bar in μm). (For interpretation of the references to color in this figure legend, the reader is referred to the web version of this article.)

conditions needed for ferrihydrite to be transformed into hematite, versus local wet conditions that permit the formation of goethite (see D'Amico et al., 2016; Fedoroff and Courty, 2013). The oxidation processes or Fe impregnation were predominant in the following soil horizons: O24014, R9, and Wd4g, and also strong in Q Inner Red, in Q Outer Red W, R1920, but less in Q Outer Red Upper and Lower, R24 Upper and Lower, and Wd5g. The yellow red-brown color more prevalent in type (2) and yellow color of type (3), suggests the presence of fine, dispersed goethite or ferrihydrite, which is also attributed to clay and Fe oxide co-illuviation, topography and climate (see D'Amico et al., 2016; Fedoroff and Courty, 2013). However, it is moderate (type 2) to low (type 3) impregnation as one can discern the calcite crystallitic groundmass.

Very rare to rare iron hypercoatings (matrix pedofeatures) covering limestone grains were found in samples Q Outer Red Upper and Lower, R24 Upper and Lower, and R1920, while slides R1920 and Wd4g lower contained iron hypercoatings in grain pores that is also associated with reddening. Secondary iron precipitations (intrusive pedofeatures) in the form of nodules or masses were found to be rare to very rare in sample Q Outer Red, while rare frequencies were observed in samples Wd5g and Wd4g.

Some important intrusive textural pedofeatures were observed in some of the samples. For example, dusty clay coatings are common in planar voids in sample Q Outer Red Upper, while similar dusty coatings are few in planar voids but common on grains in slides O24014 and R24 Upper. Very rare to rare frequencies of dusty clay coatings were observed on grains in samples Q Outer Red and Q Inner Red, Wd5g, Wd4g, R24 Lower and R9 (Fig. 4e and f). Samples Q Inner Red, R24 Upper and Lower also has some bioturbation disruption with very rare 5% excremental pedofeatures.

Many samples hold evidence for carbonate dissolution and accretion, and the samples in general displayed especially common secondary carbonate precipitation as coatings in and along planar and channel-and-chamber voids. The calcite infillings are typically mosaic xenotropic crystals manifested as dense incomplete along planar voids and loose discontinuous in channel-and-chamber voids (Fig. 4b, d, and f). In some slides, such as Q Inner Red, Q Outer Red, Wd5g and Wd4g, they are

associated with other textural pedofeatures, such as fine material coating larger grains within the fabric or in voids.

3.2.5. Cultural inclusions

All of the soil horizons, except for Q Outer yellow had cultural inclusions including bone, charcoal, mortar/plaster, ash and ceramic fragments (Figs. 6 and 7). Burnt silt-sized ceramic fragments were dispersed throughout all samples, except Q Outer Yellow, as seen with OIL light. Samples with fine charcoal fragments were observed in Trench Q, while coarse charcoal fragments were observed in Trench O, and in samples R1920 and Wd4g. Mixed fine and coarse charcoal fragments were observed in samples R24 Lower and Upper, R9 and Wd5g. Samples with slightly less charcoal include R9, Wd29 upper, Q Inner Red and Q Outer Red. Calcite shells were identified in Trenches W and O, and in some samples from Trench Q, such as Q Inner Red, and Q Outer Red Lower. Burned bone was identified in O24104. Large ceramic fragments, and mortar, and/or plaster, were found in samples R1920 and Wd29 upper, and ash was observed in R24 Upper, R1920 and Q Outer Red Lower (Figs. 6 and 7). Macro and some micro-fossils were common in R24 Upper and few in R24 Lower.

All samples contained varying amounts of subrounded, silt-sized fine, black particulate matter (BPM) within the fabric. On average, there were 144 particles counted for a grid, and they were on average 15 μm in size. Black particulate matter was few to frequent in all samples except in Wd4g and Wd5g, where there were very few to few particles, though they appeared larger than average. In sample Q Outer Yellow, the black particulate matter was rare in the upper part of the thin section. Due to the trace amounts and sporadic appearance of the BPM in the upper part of the horizon, it is suggested that they percolated down from the overlying layer (O Outer Red W). The BPM was randomly distributed in the fine matter of all samples but was also observed in the root pores of Q Inner Red, Q Outer Red Upper and Lower samples. The application of OIL light indicated that some of these silty sized particles

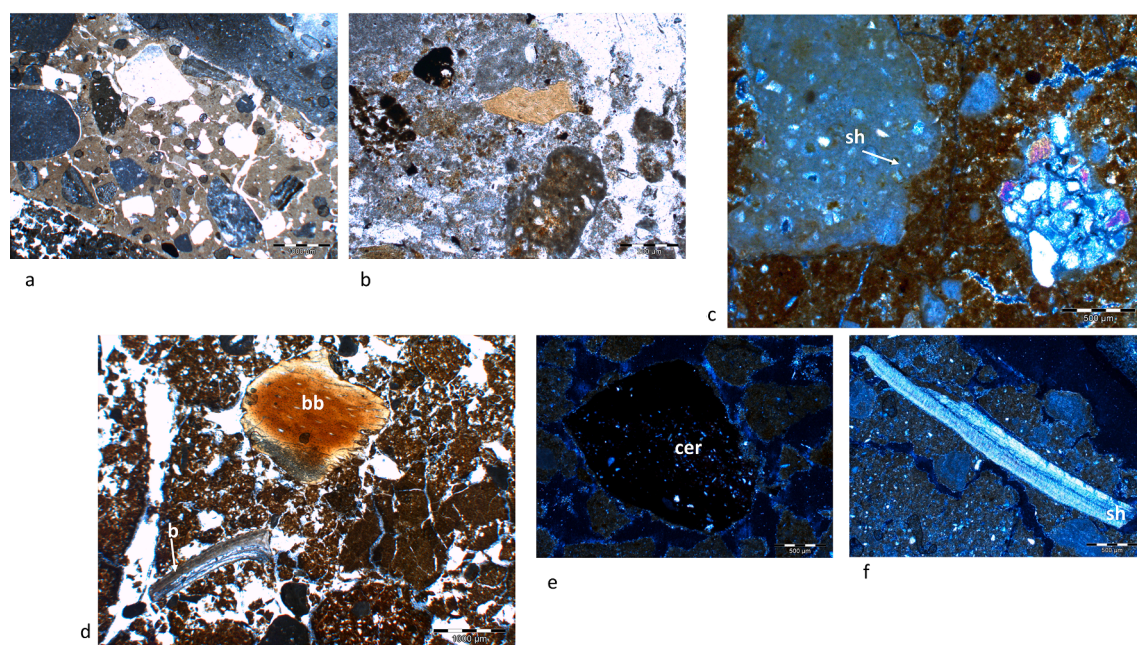


Fig. 6. Micromorphological image of cultural inclusions. 6a) Mortar R1920 with many limestone and some charcoal inclusions in slide R1920 (PPL; 1000 μm); 6b) mortar R24 (200 μm); 6c) Plaster (pl) and shell (sh) inclusions in slide Wd4g (XPL; 500 μm); 6d) burnt bone (bb) and bone fragments in sample O24014 (PPL; 500 μm); and 6e) ceramic (cer) fragment in slide Wd4g (XPL; 500 μm). 6f) shell (sh) fragment in Q Outer Red Lower (PPL). (PPL - Plane polarized light; XP - Cross polars; scale bar in μm). (For interpretation of the references to color in this figure legend, the reader is referred to the web version of this article.)

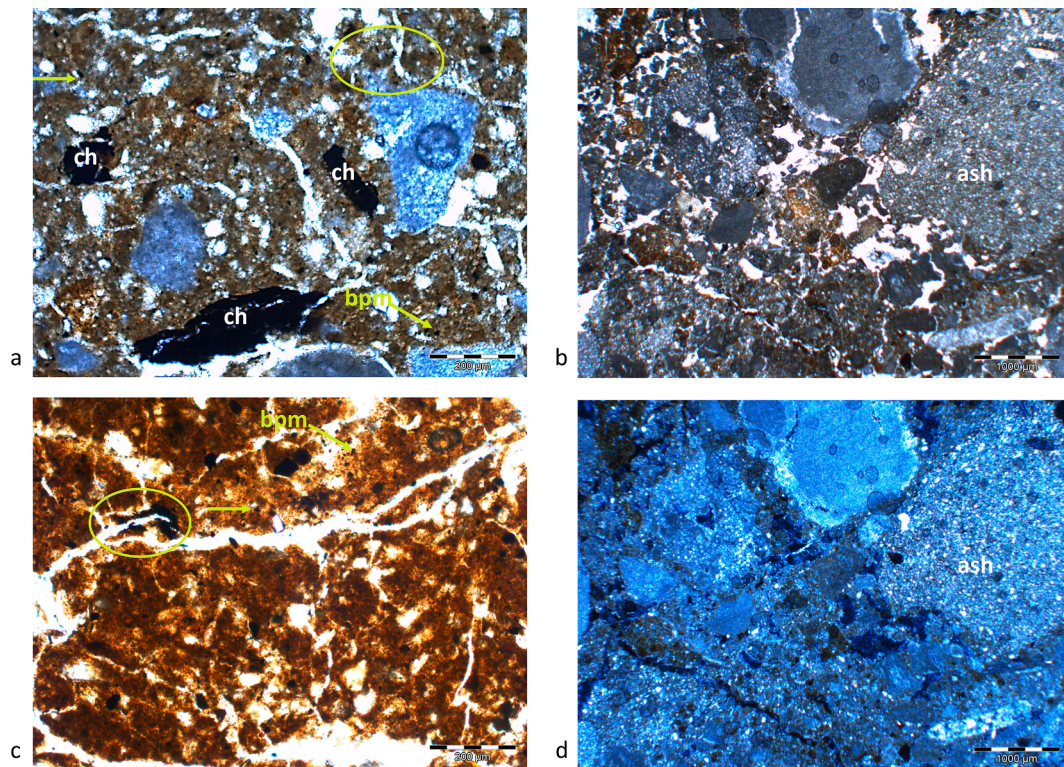


Fig. 7. Image of cultural inclusions. 7a) Charcoal fragments (ch) in Q Outer Red (PPL; 200 µm); and 7b) Ash mixed with charcoal fragments and soil fragments in R1920 (PPL; 1000 µm); 7c) in O24014 (PPL; 200 µm, where bpm also lines some voids (lime green circle); 7d) same as 7b in XPL 1000 µm). (PPL - Plane polarized light; XP - Cross polars; scale bar in µm). (For interpretation of the references to color in this figure legend, the reader is referred to the web version of this article.)

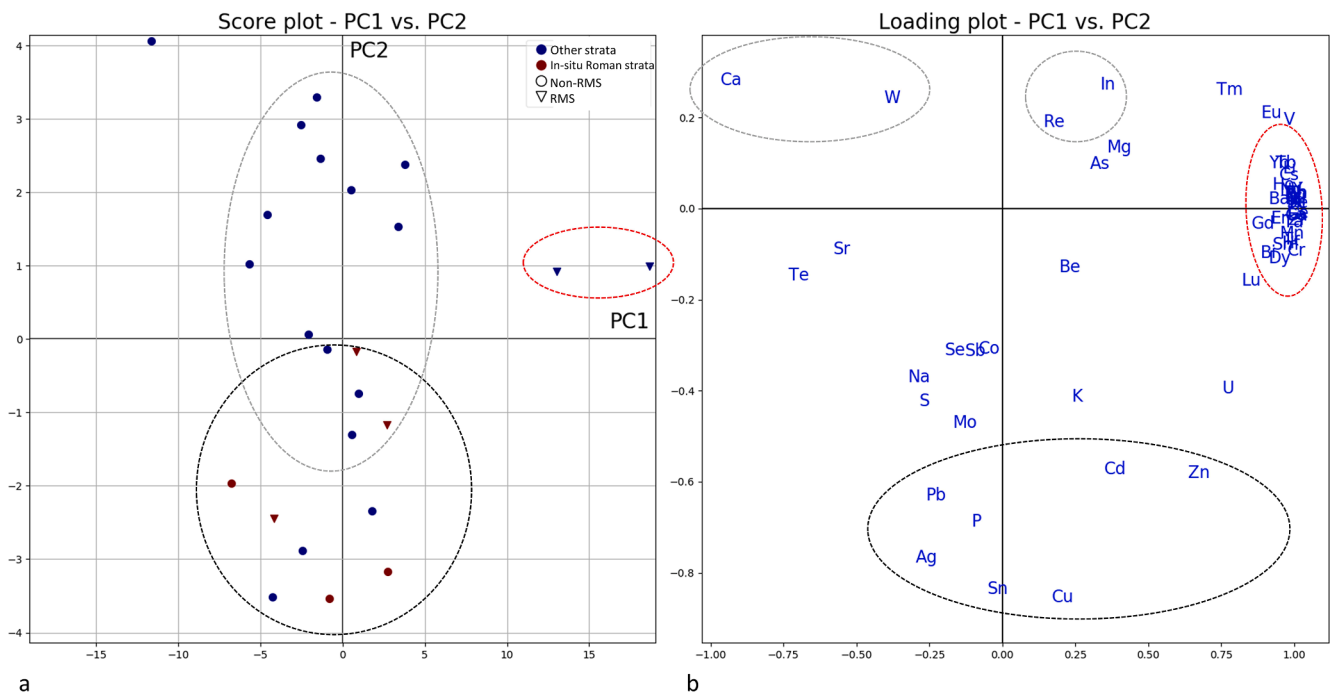


Fig. 8. Principal component analysis. 8a) score and 8b) loading plots for PC1 and PC2 for samples of various strata, including Red Mediterranean Soil (RMS) material in the Northwest Quarter, Jerash. Red color differentiates Roman aged RMS and other strata, while the triangle shape indicates RMS material versus other soil or sediments (indicated by circles). The open red dashed oval in the score plot highlights the two RMS material obtained from Trench W that likely originates from off the site. (For interpretation of the references to color in this figure legend, the reader is referred to the web version of this article.)

were burned.

3.3. Bulk soil geochemistry

The elemental concentrations of the sediments within the city and the RMS material is shown in Appendix A [Supplementary Data Table S4](#). The heavy metals of the sediments in the wadi are discussed in more detail in [Holdridge et al. \(2021\)](#). The within city RMS material had an average P content of 2000 (range 940–2930 mg/kg, $n = 5$), while the inner-city non-RMS sediments had 2060 mg/kg (range 1080–3430 mg/kg, $n = 19$). The following focus only on the PCA results of these first PCs, as the explanation power of the higher PCs is so low that it is not possible to interpret them reliably. The PCA of bulk soil geochemistry revealed that some overlap exists between RMS and other soils and sediments within the city ([Fig. 8a](#)). There is, though, a clear grouping of RMS on the score plot ([Fig. 8a](#)) which seems to be related to higher levels of Ag, Cd, Cu, P, Pb, Sn and Zn relative to the non-RMS samples which are relatively higher in Ca, Mg and some rare earth metals ([Fig. 8b](#)).

4. Discussion

4.1. Natural vs. Human-soil formation vs. Soil classification

Comparing the characteristics of the RMS samples from NWQ of Jerash with traits, typical of ‘natural’ RMS (as in [Fedoroff and Courty, 2013; Lucke et al., 2014a, 2014b; Lucke et al., 2013; Fedoroff, 1997](#)), demonstrates that these have similarities, including high clay, high amount of Fe oxides, and low organic matter. The only YMS, Q Outer Yellow, appears to have less clay and Fe oxides than the RMS, and the b-fabric illustrated the strong influence that weathered bedrock had on this soil (Appendix A, S1). The regional Cambisols as exposed in the adjacent Wadi Suf have been dated to the late Pleistocene based on OSL dating of quartz ([Lichtenberger et al., 2019](#)). Here, several of the RMS samples within the city walls were characterized by equivalent dose distributions which contain sub-populations that trend to a higher dose, which could correspond to origins in the late Pleistocene. [Lucke et al. \(2014a, 2014b\)](#) suggest that the quartz and trace amounts of silt to fine sand-sized particle additions occurred in the late Pleistocene when the climate was cooler and windier, as also suggested by others (e.g., [Fedoroff et al. 1997](#)). The origin of much of this allochthonous material came from North Africa ([Lucke et al., 2014a, 2014b](#)) and possibly also from the Arabian desert ([Kalderon-Asael et al., 2009](#)).

The evidence for clay accumulation and co-illuviation of clay and Fe oxides, aeolian input and reworking, and age difference of aeolian input and reworking ([Figs. 5 and 6](#)) is strong evidence for polygenetic development of these soils between the Pleistocene and early Holocene. The formation of RMS found within the city, involving clay illuviation and dispersion of Fe can likely be attributed to interglacial and/or interstadial periods that occurred since the Pliocene and early Pleistocene through to the terminal Pleistocene/ early Holocene (e.g., [D’Amico et al., 2016; Fedoroff, 1997](#)). Other processes like natural erosion, aeolian disruption, and aggradation are thought to have occurred during Glacial periods and stadials (e.g., [Fedoroff, 1997](#)). [Fedoroff \(1997\)](#) showed that the location and disassociation of clay coatings and carbonates meant that they formed at different times, the former in humid and warm, interglacial/interstadial climates, and the latter in glacial and stadial cooler and drier climates. Thus, carbonate coatings, observed in the planar and channel-and-chamber voids in all our samples ([Supplementary Data Table S1](#)) may be related to the inherited fabric of the soil.

In the wadi, OSL ages on some of the RMS material provided ages corresponding to the early Holocene, suggesting reworked RMS accumulated as Fluvisols adjacent to the wadi in relation to past climatic conditions or climate change, and/or possibly local human (e.g. Neolithic) impact (see [Fedoroff, 1997; Holdridge, submitted; Lichtenberger et al., 2019](#)). The reworking is characteristic of some RMS, which

are essentially defined as pedo-sedimentary complexes ([Durn, 2003; Federoff, 1997](#)).

The major differences in structure, fabric, sorting and textural pedofeatures, and in particular inclusions in the RMS at Jerash as compared to ‘natural’ RMS described in many studies can likely be attributed to human activities. The sample, Q Outer Yellow, obtained from just outside the city wall, was the only thin-section sample studied that indicated very minor impacts by human activities (e.g., at the very top, infiltration of silt-sized particles from above), but appears to be dominated by natural RMS processes. This sample will not be discussed below except where specifically mentioned as a reference.

4.2. RMS material on the site of Jerash

4.2.1. Ages on-site

According to the OSL ages in Trenches R, O and Q at Jerash ([Table 1](#)), there is indication that the RMS had formed before 1000 BCE in the Iron Age or pre-Hellenistic period. The weighted combination of the RMS samples, assuming similar depositional histories and attributes, would suggest disturbance of the soil surface certainly by 270 ± 90 BC (SUTL2876, 2878 and 2881; [Cresswell et al., 2017](#)). Further evidence for initial disturbance in the Hellenistic period is suggested by a quartz SAR OSL age of 480 ± 280 BCE (SUTL2880; [Cresswell et al., 2017](#)) for the soil in Trench Q, which, according to literary sources, coincided with the period when the city was re-founded ([Raja 2012](#)), and when the natural surface soil was likely used, eroded and incorporated into the urban fabric as the site expanded. Many of our RMS samples contain Roman finds (data not shown) and are therefore also associated with activity during the Roman period. Combined this suggests that the human impact manifested by the RMS are a mix of initial disturbances during the Hellenistic period and later disturbances during Roman times that were related to the establishment and growth of the city including deforestation, construction, quarrying for building material, and possibly some cultivation within the city. Samples R9, R1920, Wd5g and Wd4g are associated with Byzantine finds and reflect later human activities.

4.2.2. Within city agriculture and gardening?

Based on the micromorphological evidence in section 3 we suggest that the human influenced or ‘non-natural’ characteristics of the majority of RMS from the NWQ reflects gardening activities or similar intensive management and cultivation practices within the city area. As almost no macro- (except in R24) or micro-fossils such as pollen or phytoliths were preserved in any of the soil horizons, it added to the complexity of interpreting our results. Some traits of human influenced pedogenesis, such as textural pedofeatures in combination with soil mixing and fragmentation, are indicative of low intensity agriculture with no or little manuring ([Macphail and Goldberg, 2017; 341](#)). However, the various types and amounts of mineral and organic cultural

Table 1

Quartz SAR OSL depositional ages for Red Mediterranean Soil. Further details in [Supplementary Data Methods in Cresswell et al. \(2017\)](#).

SUTL no.	Trench ID, Context no.	Dose rate/ mGy a ⁻¹	Stored dose/Gy	Age/ka	Calendar years
2876	O [104]	2.16 ± 0.11	4.98 ± 0.07	2.31 ± 0.13	300 ± 130 BCE
2879	R [9]	1.49 ± 0.09	9.74 ± 2.96	6.56 ± 2.03	4540 ± 2030 BCE
2878	R [24]	1.36 ± 0.11	3.10 ± 0.05	2.27 ± 0.18	260 ± 180 BCE
2877	R [29]	0.71 ± 0.04	2.16 ± 0.06	3.02 ± 0.20	1010 ± 200 BCE
2880	Q Inner	1.59 ± 0.07	3.97 ± 0.41	2.50 ± 0.28	480 ± 280 BCE
2881	Q Outer	1.18 ± 0.07	9.85 ± 3.02	8.35 ± 2.60	6330 ± 2600 BCE

inclusions observed in all samples are materials found incorporated into intensively farmed soils such as both gardens and agricultural fields (see Macphail and Goldberg, 2017). In particular, randomly distributed and strongly fragmented charcoal, pottery, bone and ash from kitchen waste (Figs. 5 and 6) are highly suggestive of soil manuring and cultivation (Wouters et al., 2017; Simpson et al., 1998; Simpson et al., 2000; Vissac, 2005). Furthermore, enhanced levels of P, an indicator of organic amendment, found in some of the RMS relative to average within-city sediments despite the fact that RMS had a lower average (2070 vs. 2450 mg P/kg, respectively, See Appendix A, Table S4), but significantly higher P levels than any soil or sediment found upstream of the city (Holdridge et al., 2021). This also supports the view that these soils were part of an ancient agricultural system.

In addition, samples contained well-rounded clasts, suggesting that they do not derive from slope-wash, but instead originate from ancient fluvial deposits found in the landscape along the Wadi Suf terraces. Even though colluvial inclusions including slope-wash are indicative of agriculture effects of clearing and agriculture (Macphail and Goldberg, 2017), in this case it may be a deliberate cultural inclusion. According to Roman authors, clay was mixed with gravel in order to obtain a good consistency for the soil (Farrar et al., 1998). Carbonate dissolution/accretion has also been associated with the evaporation of soil water and wetting and drying in relation to agriculture (as in Gilliland et al., 2013; Stoops, 2013), and may possibly be another strand of evidence to support agricultural-related activities within the city. The combination of contrasting fabrics pedogenic indicators, and enhanced P values indicates a cultivated surface on which inclusions are predominantly culturally deposited rather than reworked.

The case for gardening/horticulture and possibly cultivation is very strong in samples Q Outer Red, O24104 and R24 Upper and Lower. In the Q Outer Red and O24104 samples the microscale-scale patterning and sorting of quartz grains, the well-sorted fine silt/clay accumulations and the associated micro-cultural debris are indicative of irrigation. The proximity of Trench O to the cistern as well as the evidence for organic waste, mixed fabrics and fragmented peds, textural pedofeatures in samples O24104 all point to the use of the within city site for cultivation (as in Macphail and Goldberg, 2017). Sample Q Outer Red was obtained from an outdoor space just inside the city wall, and with similar evidence as that in O, it implies that this area was also used for cultivation. In the samples R24 Upper and Lower, the evidence for fragmented plant inclusions in conjunction with textural pedofeatures and fragmented peds, strongly signals horticultural practices and processing of plant material in an outdoor space on-site during the Roman period. Evidence from the other Trench Q samples taken from just outside the city wall, which are also interpreted as outdoor spaces, suggests that they were agriculturally disturbed and modified soils, but it appears to have been less intense or to have undergone a different management than inside the city wall (e.g., especially as observed contrasts in Q Outer Red, R24 Upper and Lower, and in Trench O). Soils external to the wall all contained overall less cultural inclusions, and less pedofeatures, mixed fabric and fragmented peds.

Part of the complexity in interpreting the RMS material from Trenches R (R1920 and R9) and W is due to their origin as disturbed, ex-situ material. The archaeological interpretations of Trenches R (samples R1920, R9) and W (Wd5g and Wd4g) characterize them as outdoor spaces. The movement or transportation of material either within site (e.g., in Trench R) or from off-site locations (e.g., Trench W) strongly suggests that this material served an intended purpose. Since RMS is one of the more fertile soil types in Jordan (Lucke et al., 2013), and as RMS material is still transported and used for contemporary gardening (see Fig. 2c,f), this suggests that RMS was imported on-site for gardening purposes (albeit not necessarily exclusively) during the Byzantine to Umayyad periods (e.g., Trench R) and Byzantine periods (e.g., Trench W).

The evidence, e.g. textural pedo-features and cultural inclusions in samples R9 and Wd5g and Wd4g, is similar to that in RMS samples found

beneath the city wall (Q Outer Red Upper and Lower, and Q Inner Red). However, their location on-site may suggest that the former samples represent more of a decorative garden versus horticulture, which could have involved different types of plants and/or management. Conversely, the lack of textural pedo-features in sample R1920 in conjunction with large fragmented, diverse cultural material is more suggestive of an unmanaged space with increased accumulation of occupational debris.

In relation to Trench W, Fig. 8 (outlined by red dashed oval) and 10 show that it is clearly different from other strata on-site as it contains high amounts of rare earth elements, which do occur in Cretaceous Phosphorites (Abed and Abu Murry, 1997) and other Cretaceous rocks (El-Hasan et al., 2008), in Jordan. Though, more analyses would be needed to determine the origin of the soil material in Trench W, as various materials rich in rare earth elements have been used as fertilizer in East Asia (Tyler, 2004). It may be that the space changed from a garden to an open urban occupational space over time (as in Wouters et al., 2017; Davidson et al., 2006) though as original RMS surfaces are rarely preserved (or observed until now) in Jerash that temporal fluctuations in their use cannot be established. Similar, heterogeneous finds in an historic garden were associated with a pathway through that garden (as in Vissac, 2005), which also may be the case here. Gardening seems to be an aspect of the inner-city land-use in ancient Gerasa/Jerash, and production gardening could hence not only be important for understanding urban resilience in a historical perspective, but also for future strategies for sustaining a high level of food-security as cropland globally disappears and urban areas sprawl (Bren D'Amour et al., 2016).

4.3. Contamination of past urban RMS

The silt-sized black particulate matter or black carbon, which is observed in all samples except sample Q Outer Yellow (Figs. 6 and 7), are results of the incomplete combustion of biofuels including wood and animal dung during ancient times, and more recently, fossil fuels (Schmidt and Noack, 2000). The production of black carbon (also known as biochar) has various origins including natural forest fires, and urban domestic, industrial and artisanal activities, the latter involving metal, ceramic, and glass production including polycyclic aromatic hydrocarbons and graphitic moieties (He and Zhang, 2009; Schmidt and Noack, 2000). These produce stable aromatic components within the soil organic matter that resist decomposition, lasting for millennia or more in soils (Schmidt and Noack, 2000). Black carbon becomes a part of the soil due to in-situ processes (e.g. burning) or via fluvial and aeolian processes (Schmidt and Noack, 2000). For example, micromorphological and geochemical analyses of rural soils in northern Europe indicated that black carbon reached the soils via aeolian processes having derived from peat fires in a nearby 17th to 19th urban center (Davidson et al., 2006). Conversely, evidence for an in-situ relationship between black carbon and metalworking has been observed since the 3rd-6th centuries AD, with a peak in the 13-14th centuries AD in China (He and Zhang, 2009). In this study, the evidence points to the origin of the black carbon in the urban RMS due to the burning of organic material for various inner city activities, which reached and were incorporated into the soils via aeolian and water erosion processes.

Referring to Fig. 8, comparing the black dashed circle that encloses the Roman strata and RMS as well as some other strata to the loading plot suggests that they are influenced by high amounts of the elements Pb, P, Sn, Cu, Ag, Zn and Cd (black dashed oval), many of which result from human activities (Sulas et al., 2019) such as smelting working. Some of the other strata appear to be influenced more by Ca, W, Re and In, though it is unclear why (see light grey black dashed oval/circles on both plots).

Based on both geochemical analyses and bulk geochemistry, the heavy metal distribution comprises diffuse heavy metal concentrations throughout the fine matter/groundmass of the RMS, which were former surfaces, used for horticulture over a period of time. In present day studies of heavy metal distribution in urban soils, it was found that

increased metal concentrations in surface horizons may have resulted from irrigating soils with waste water containing contaminants (Van Oort et al., 2008). In summary, the urban RMS at Jerash, like contemporary urban soils, served as sinks of contaminants including Pb, Cu, and P, the sources of which resulted from urban industrial, farming and artisanal activities (Holdridge et al., 2021). Novel methods are nevertheless needed for future studies of ancient gardening on RMS in the region, e.g. biomarkers for identification of faeces and plant remains, in particular as pollen and phytoliths seem to be poorly preserved (Bugge et al., 2015).

5. Conclusions

Comparing the results of the samples to macro and micromorphology studies of other RMS and other soils in urban environments demonstrates that the RMS material found in the Northwest Quarter in Jerash has both natural and anthropogenic components. Comparing these soils to modern urban settings suggests that human activities modified soil material fabrics, contributed to textural pedofeatures formation and resulted in additions to the soil including artifacts and waste including contaminants/pollutants (Amosse et al., 2015; Yang and Zhang, 2015; Scharenbroch et al., 2005). In particular, one of the main evidences supporting their urban nature was the fact that they have enhanced levels of Pb, Cu and Sn, which derive from industrial and/or artisanal activities that were incorporated into the soil via aeolian and/or surface water erosion processes. The relative intensities of use of RMS material for urban gardens (horticulture) and possibly larger scale intensive cultivation in Jerash is reflected in the amount and variety of finds as compared to the relative lack of finds (e.g. except for a fragment of pottery) in rural settings in the Mediterranean (French and Whitelaw, 1999). The RMS material represents a very fertile soil present in the region, and the context and human impact on the RMS material at Jerash strongly indicates that it was used for cultivation and/or urban gardens from the Roman into the Umayyad period. Urban gardens and larger scale intensive cultivation in conjunction with water management are emerging as a vital element of food security, adaptations to environmental change and long-term urban development in ancient Jerash (Stott et al., 2018; Kristiansen and Stott, 2020; Lichtenberger and Raja, 2019). It is also evident from early urban areas in other regions of the world that targeted inner city use of RMS for gardens and/or orchards has contributed to longevity and resilience over extended periods of time (Barthel and Isendahl, 2013; Kristiansen, 2018). As well as highlighted early urban garden practices in the Eastern Mediterranean, our study offers new high-resolution soils-based approaches that disentangles natural and cultural soil forming processes, and may identify and assess the creation, fertility, management and unintended changes in early urban gardens in different regions.

Declaration of Competing Interest

The authors declare that they have no known competing financial interests or personal relationships that could have appeared to influence the work reported in this paper.

Acknowledgements

This research was undertaken within the framework of the Danish-German Jerash Northwest Quarter Project of the Universities of Aarhus and Münster. We thank the Department of Antiquities in Amman and Jerash for their support. Thanks are also due to the funding bodies supporting the project: the Carlsberg Foundation, the Danish National Research Foundation (grant 119), the Deutsche Forschungsgemeinschaft, the Deutscher Palästina-Verein, the Danish EliteForsk Award and H. P. Hjerl Hansens mindefondet for Dansk Palæstinaforskning. Financial support for the OSL analyses was provided by the Scottish Alliance for Geoscience, Environment and Society

(SAGES). We thank Thomas Ljungberg for help with illustrations and Python scripts.

Appendix A. Supplementary material

Supplementary data to this article can be found online at <https://doi.org/10.1016/j.jasrep.2022.103633>.

References

- Abed, A.M., Abu Murry, O.S., 1997. Rare earth element geochemistry of the Jordanian Upper Cretaceous Phosphorites. *Arab Gulf J. Sci. Res.* 15, 41–158.
- Adderley, W.P., Wilson, C.A., Simpson, I.A., Davidson, D.A., 2018. Anthropogenic Features. In: Stoops, G., Marcelino, V., Mees, F. (Eds.), *Interpretation of Micromorphological Features of Soils and Regoliths*, 2nd Edition. Elsevier, Amsterdam, pp. 753–778.
- Al-Eisawi, D.M., 1985. Vegetation of Jordan. In: Hadidi, A. (Ed.), *Studies in The History and Archaeology of Jordan II*. Ministry of Archaeology, Amman, pp. 45–57.
- Al-Qudah, B., 2001. Soils of Jordan. Soil resources of southern and eastern Mediterranean countries. CIHEAM-IAMB, Bari, pp. 127–141.
- Amossé, J., Le Bayon, R.C., Gobat, J.M., 2015. Are urban soils similar to natural soils of river valleys? *J. Soils Sediments* 15 (8), 1716–1724.
- Awadh, S.M., 2012. Geochemistry and mineralogical composition of the airborne particles of sand dunes and dust storms settled in Iraq and their environmental impacts. *Environ. Earth Sci.* 66 (8), 2247–2256.
- Barthel, S., Isendahl, C., 2013. Urban gardens, agriculture, and water management: Sources of resilience for long-term food security in cities. *Ecol. Econ.* 86, 224–234.
- Bedal, L.-A., Conyers, L.B., Foss, J.E., Gleason, K.L., 2013. The Petra Garden and Pool Complex, Ma'an Jordan. In: Malek, A.-A. (Ed.), *Sourcebook for garden archaeology: methods, techniques, interpretations and field examples*. Lang, Bern, pp. 625–642.
- Bender, F., 1974. *Geology of the Arabian Peninsula*, Jordan. Report Number: 74-215 Reston, VA: U. S. G. Survey.
- Bogaard, A., 2005. 'Garden agriculture' and the nature of early farming in Europe and the Near East. *World Archaeol.* 37 (2), 177–196.
- Boyer, D.D., 2018. The Role of Landscape in the Occupational History of Gerasa and its Hinterland, in: Lichtenberger, A., Raja, R. (Eds.), *The Archaeology and History of Jerash*. 110 Years of Excavations, Turnhout, p. 59–86.
- Bren d'Amour, C., Reitsma, F., Baiocchi, G., Barthel, S., Güneralp, B., Erb, K.-H., Haberl, H., Creutzig, F., Seto, K.C., 2016. Future urban land expansion and implications for global croplands. *Proc. Natl. Acad. Sci. USA* 114 (34), 8939–8944.
- Bugge, B., Wiesenberg, G., Eglinton, T., Lucke, B., 2015. Molecular proxies in Late Holocene soils and sediments of Jordan - Principles, Potentials and Perspectives. In: Lucke, B., Bäumler, R., Schmidt, M. (Eds.), *Soils and Sediments as Archives of Environmental Change. Geoarchaeology and Landscape Change in the Subtropics and Tropics*, Fränkische Geographische Gesellschaft, Erlangen, pp. 163–182.
- Bullock, S., Fedoroff, N., Jongerius, A., Stoops, G., Turisna, T., 1985. Handbook for soil thin section description. Wayne Research Publications, Wolverhampton.
- Cato the Elder), De Agricultura, 1. English translation from: http://penelope.uchicago.edu/Thayer/E/Roman/Texts/Cato/De_Agricultura/A*.html.
- Columella, Lucius Junius Moderatus, volume 1 (I-IV) translated by Ash, H. B. 1941. Harvard University Press: Cambridge. AD 70.
- Cresswell, A.J., Sanderson, D.C.W., Kinnaird, T.C., Holdridge, G., Lichtenberger, A., Raja, R., Simpson, I., 2017. Luminescence dating of soils and sediments from Jerash. Jordan. *Jerash Geoarchaeology Working Paper*. <http://hdl.handle.net/1893/27524>.
- D'Amico, M.E., Catoni, M., Terribile, F., Zanini, E., Bonifacio, E., 2016. Contrasting environmental memories in relict soils on different parent rocks in the south-western Italian Alps. *Quat. Int.* 418, 61–74.
- Davidson, D.A., Dercon, G., Stewart, M., Watson, F., 2006. The legacy of past urban waste disposal on local soils. *J. Archaeol. Sci.* 33 (6), 778–783.
- Delgado, R., Martín-García, J.M., Calero, J., Casares-Porcel, M., Tito-Rojó, J., Delgado, G., 2007. The historic man-made soils of the Generalife garden (La Alhambra, Granada, Spain). *Eur. J. Soil Sci.* 58 (1), 215–228.
- Devos, Y., Nicosia, C., Vrydaghs, L., Speleers, L., Van der Valk, J., Marinova, E., Claes, B., Albert, R.M., Esteban, I., Ball, T.B., Court-Picon, M., 2017. An integrated study of Dark Earth from the alluvial valley of the Senne river (Brussels, Belgium). *Quat. Int.* 460, 175–197.
- Durand, N., Monger, H.C., Canti, M.G., 2010. Calcium Carbonate Features. In: Stoops, G., Marcelino, V., Mees, F. (Eds.), *Interpretation of Micromorphological Features of Soils and Regoliths*, 1st Edition. Elsevier, Amsterdam, pp. 149–194.
- Durn, G., 2003. Terra rossa in the Mediterranean region: parent materials, composition and origin. *Geologia Croatica* 56 (1), 83–100.
- El-Hasan, T., Al-Malabeh, A., Komuro, K., 2008. Rare Earth Elements geochemistry of the Cambrian shallow marine manganese deposit at Wadi Dana, south Jordan. *Jordan J. Earth Environ. Sci.* 1 (1), 45–52.
- Esbensen, K.H., 2004. Multivariate data analysis: in practice: an introduction to multivariate data analysis and experimental design, 5th Edition. Camo Process AS, Woodbridge.
- Farrar, L., 1998. *Ancient Roman Gardens*. Sutton Publishing Limited, Phoenix Mill.
- Fedoroff, N., 1997. Clay illuviation in red Mediterranean soils. In: Mermut, A.R., Yaalon, D.H., Kapur, S. (Eds.), *Red Mediterranean Soils*. Catena, vol. 28, pp. 171–189.
- Fedoroff, N., Courty, M.A., 2013. Revisiting the genesis of red Mediterranean soils. *Turk. J. Earth Sci.* 22, 359–375.

- French, C.A., Whitelaw, T.M., 1999. Soil erosion, agricultural terracing and site formation processes at Markiani, Amorgos, Greece: the micromorphological perspective. *Geochronology* 14 (2), 151–189.
- Gilliland, K., Simpson, I.A., Adderley, W.P., Burbidge, C.I., Cresswell, A.J., Sanderson, D.C., Coningham, R.A.E., Manuel, M., Strickland, K., Gunawardhana, P., Adikari, G., 2013. The dry tank: development and disuse of water management infrastructure in the Anuradhapura hinterland, Sri Lanka. *J. Archaeol. Sci.* 40 (2), 1012–1028.
- He, Y., Zhang, G.L., 2009. Historical record of black carbon in urban soils and its environmental implications. *Environ. Pollut.* 157 (10), 2684–2688.
- Holdridge, G., 2020. The Geology of the Northwest Quarter of Ancient Jerash within its Regional Context. In: R. Raja, A. Lichtenberger (Eds.): Chapter 2. Jerash Papers. Turnhout, Brepols.
- Holdridge, G. submitted. City and Wadi: long-term human impacts on eastern Mediterranean sediment dynamics at a catchment scale. *Geomorphology*.
- Holdridge G., Kristiansen, S.M., Raja R., Lichtenberger, A., Simpson, I.A., 2020. Soils, sediments and urban history: introducing geosciences to the archaeology at Jerash. In: R. Raja, Lichtenberger, A. (Eds.). Chapter 3. Jerash Papers. Turnhout, Brepols.
- Holdridge, G., Kristiansen, S.M., Barford, G.H., Lichtenberger, A., Olsen, J., Philippsen, B., Raja, R., Kinnaird, T., Simpson, I.A., 2021. A Roman provincial city and its contamination legacy from artisanal and daily-life activities. *PLoS ONE*. <https://doi.org/10.1371/journal.pone.0251923>.
- Homsher, R.S., Tepper, Y., Drake, B.L., Adams, M.J., David, J., 2016. From the bronze age to the “lead age”: Observations on sediment analyses at two archaeological sites in the Jezreel Valley, Israel. *Mediterranean Archaeology and Archaeometry* 16 (1), 187–204.
- Ishawari, A. (2013). *Identification chart for the rock-forming minerals by polarizing microscope*. The Geological Society of Japan - Meiji Techno Co., Ltd.
- Horváth, A., Szita, R., Bidló, A., Gribovszki, Z., 2016. Changes in soil and sediment properties due the impact of the urban environment. *Environ. Earth Sci.* 75 (17), 1211.
- Jones, G., 2005. Garden cultivation of staple crops and its implications for settlement location and continuity. *World Archaeol.* 37, 164–176.
- Kalaitzoglou, G., Lichtenberger, A., Raja, R., 2015. Preliminary report on the fourth season of the Danish-German Jerash Northwest Quarter Project 2014. *Annual of the Department of Antiquities of Jordan*, 59.
- Kalderon-Asael, B., Erel, Y., Sandler, A., Dayan, U., 2009. Mineralogical and chemical characterization of suspended atmospheric particles over the east Mediterranean based on synoptic-scale circulation patterns. *Atmos. Environ.* 43 (25), 3963–3970.
- Kristiansen, S.M., 2018. In: Gardening and food security in early southern-Scandinavian urbanism: Existing evidence and the need for a high-definition approach. In: *Urban network evolution – towards a high definition archaeology*. Aarhus University Press, Aarhus, pp. 255–259.
- Kristiansen, S.M., Stott, D., 2020. Mapping Jerash by Remote Sensing. In: Raja, R., Lichtenberger, A. (Eds.). Chapter 8. Jerash Papers. Turnhout, Brepols.
- Lehmann, A., Stahr, K., 2007. Nature and significance of anthropogenic urban soils. *J. Soils Sediments* 7 (4), 247–260.
- Lichtenberger, A., Raja, R., 2015. New Archaeological Research in the Northwest Quarter of Jerash and Its Implications for the Urban Development of Roman Gerasa. *Am. J. Archaeol.* 119 (4), 483–500.
- Lichtenberger, A., Raja, R., 2018a. Middle Islamic Jerash through the lens of the Longue Durée. In: *Middle Islamic Jerash (9th – 15th century) Archaeology and History of an Ayyubid-Mamluk Settlement*. Jerash Papers 3. Eds. Lichtenberger, A. and Raja, R. (Turnhout: Brepols), 5–36.
- Lichtenberger, A., Raja, R., 2019. Defining Borders: The Umayyad-Abbasid Transition and the Earthquake of AD 749 in Jerash. In: *Byzantine and Umayyad Jerash reconsidered. Transitions, Transformations, Continuities*. Jerash Papers 4. Eds. Lichtenberger, A. and Raja, R. (Turnhout: Brepols), 265–286.
- Lichtenberger, A., Raja, R., 2018b. From Synagogue to Church. The Appropriation of the Synagogue of Gerasa/Jerash under Justinian. In: *Jahrbuch für Antike und Christentum* 61, 85–100.
- Lichtenberger, A., Raja, R., 2020. Management of water resources over time in semiarid regions: The case of Gerasa/Jerash in Jordan. *WIREs. Water* e1403, 1–19.
- Lichtenberger, A., Lindroos, A., Raja, R., Heinemeier, K., 2015. Radiocarbon Analysis of Mortar from Roman and Byzantine Water Management Installations in the Northwest Quarter of Jerash, Jordan. *J. Archaeol. Sci.: Reports* 2, 114–127.
- Lichtenberger, A., Raja, R., Seland, E.H., Kinnaird, T.C., Simpson, I.A., 2019. Urban-Riverine Hinterland Synergies in Semi-Arid Environments: Millennial-Scale Change, Adaptations, and Environmental Responses at Gerasa/Jerash. *Journal of Field Archaeology* 44 (5), 333–351.
- Lucke, B., Ziadat, F., Taimed, A., 2013. The Soils of Jordan. In: *Atlas of Jordan. History, Territories and Society*. Chapter: The Soils of Jordan Publisher: Institut Français de Proche Orient, pp. 72–76.
- Lucke, B., Kemnitz, H., Baumler, R., Schmidt, M., 2014a. Red Mediterranean Soils in Jordan: New insights in their origin, genesis, and role as environmental archives. *Catena* 112, 4–24.
- Lucke, B., Ziadat, F., Taimed, A., 2014. The soils of Jordan. *Atlas of Jordan, History, Territories and Society*. (Ed. M. Ababsa.) (Presses de l'Institut Français du Proche-Orient: Beirut, Lebanon.) Available at: <http://books.openedition.org/ifpo/4867> (accessed 13 May 2017).
- Lucke, B., Kemnitz, H., Baumler, R., 2012. Evidence for isovolumetric replacement in some Terra Rossa profiles of northern Jordan. *Boletín de la Sociedad Geológica Mexicana* 64 (1).
- Martin-García, J.M., Aranda, V., Gamiz, E., Bech, J., Delgado, R., 2004. Are Mediterranean mountains Entisols weakly developed? The case of orthents from Sierra Nevada (Southern Spain). *Geoderma* 118, 115–131.
- Macphail, R.I., Goldberg, P., 2017. *Applied soils and micromorphology in archaeology*. Cambridge University Press.
- McDougall, R., Kristiansen, P., Rader, R., 2019. Small-scale urban agriculture results in high yields but requires judicious management of inputs to achieve sustainability. *Proc. Natl. Acad. Sci.* 116, 129–134.
- Merino, E., Banerjee, A., 2008. Terra Rossa Genesis, Implications for Karst, and Eolian Dust: A Geodynamic Thread. *J. Geol.* 116, 62–75.
- Muhs, D.R., Budahn, J., Avila, A., Skipp, G., Freeman, J., Patterson, D., 2010. The role of African dust in the formation of Quaternary soils on Mallorca, Spain and implications for the genesis of Red Mediterranean soils. *Quat. Sci. Rev.* 29, 2518–2543.
- Nicosia, C., Langohr, R., Mees, F., Arnoldus-Huyzendveld, A., Bruttini, J., Cantini, F., 2012. *Geochronology* 27, 105–122.
- Pereira, P., Ferreira, A., Pariente, S., Cerda, A., Walsh, R.P.D., Keesstra, S., 2016. Preface: Urban soils and sediments. *J. Soils Sediments* 16 (11), 2493–2499.
- Passchier, C., Sümmelindi, G., Boyer, D., Yalçın, C., Spötl, C., Mertz-Kraus, R., 2021. The aqueduct of Gerasa – Intra-annual palaeoenvironmental data from Roman Jordan using carbonate deposits. *Palaeoclimatology, Palaeoecology, Palaeogeography*, p. 562.
- Philippsen, B., Olsen, J., 2020. Radiocarbon dating Jerash. In: Lichtenberger, A., Raja, R. (Eds.): *The Danish-German Jerash Northwest Quarter Project. Final publications vol. 1. Environmental studies, remote sensing and modelling* (Brepols: Turnhout).
- Priori, S., Costantini, E.A.C., Capezzuoli, E., Protano, G., Hilgers, A., Sauer, D., Sandrelli, F., 2008. Pedostratigraphy of Terra Rossa and Quaternary geological evolution of a lacustrine limestone plateau in central Italy. *J. Plant Nutr. Soil Sci.* 171, 509–523.
- Price, D., Bar-Yosef, T.O., 2011. The origins of agriculture: New data, new ideas. *Current Anthropology* 52 (SUPPL. 4), S163–S174.
- Raja, R., 2012. Urban Development and Regional Identity in the Eastern Roman Provinces, 50 BC – AD 250: Aphrodisias. Museum Tusculanum Press, Ephesos, Athens, Gerasa (Copenhagen), p. 273 pp.
- Sandler, A., Meunier, A., Velde, B., 2015. Mineralogical and chemical variability of mountain red/brown Mediterranean soils. *Geoderma* 239, 156–167.
- Scharenbroch, B.C., Lloyd, J.E., Johnson-Maynard, J.L., 2005. Distinguishing urban soils with physical, chemical, and biological properties. *Pedobiologia* 49, 283–296.
- Schmidt, M., Lucke, B., Baumler, R., Al-Saad, Z., Al-Qudat, B., Hutcheon, A., 2006. The Decapolis region (Northern Jordan) as historical example of desertification? Evidence from soil development and distribution. *Quat. Int.* 151, 74–86.
- Schmidt, M.J., Rapp Py-Daniel, A., de Paula Moraes, C., Valle, R.B.M., Caromano, C.F., Teixeira, W.G., Barbosa, C.A., Fonseca, J.A., Magalhães, M.P., Silva do Carmo Santos, D., da Silva e Silva, R., Guapindaia, V.L., Moraes, B., Lima, H.P., Neves, E.G., Heckenberger, M.J., 2014. Dark earths and the human built landscape in Amazonia: a widespread pattern of anthrosol formation. *J. Archaeol. Sci.* 42, 152–165.
- Schmidt, M.W., Noack, A.G., 2000. Black carbon in soils and sediments: analysis, distribution, implications, and current challenges. *Global Biogeochem. Cycles* 14, 777–793.
- Simpson, I.A., Perdikaris, S., Cook, G., Campbell, J.L., Teesdale, W.J., 2000. Cultural sediment analyses and transitions in early fishing activity at Langenesværet, Vesterålen, Northern Norway. *Geochronology*. *Int. J.* 15, 743–763.
- Simpson, I.A., Dockrill, S.J., Bull, I.D., Evershed, R.P., 1998. Early anthropogenic soil formation at tofts Ness, Sanday, Orkney. *J. Archaeol. Sci.* 25, 729–746.
- Šmejda, L., Hejman, M., Horák, J., Shai, I., 2018. Multi-element mapping of anthropogenically modified soils and sediments at the Bronze to Iron Ages site of Tel Burna in the southern Levant. *Quat. Int.* 483, 111–123.
- Solomon, D., Lehmann, J., Leach, M., Fraser, J., Amanor, K., Frausin, V., Kristiansen, S.M., Millimouno, D., Fairhead, J., 2016. Indigenous African Soil Enrichment as Climate-smart sustainable agriculture alternative. *Front. Ecol. Environ.* 14, 71–76.
- Stoops, G., 2003. Guidelines for analysis and description of soil and regolith thin sections. Soil Science Society of America Inc.
- Stott, D., Kristiansen, S.M., Lichtenberger, A., Raja, R., 2018. Mapping an ancient city with a century of remotely sensed data. *Proc. Natl. Acad. Sci.* 115 (24), E5450–E5458.
- Sulas, F., Kristiansen, S.M., Wynne-Jones, S., 2019. Soil geochemistry, phytoliths and artefacts from an early Swahili daub house, Unguja Ukuu, Zanzibar. *J. Archaeol. Sci.* 103, 32–45.
- The Filaha Texts Project (<http://www.filaha.org/>). Homepage visited on May 15th 2022.
- Tyler, G., 2004. Rare Earth Elements in soil and plant systems- a review. *Plant Soil* 267, 191–206.
- Van Oort, F., Jongmans, A.G., Lamy, I., Baize, D., Chevallier, P., 2008. Impacts of long-term waste-water irrigation on the development of sandy Luvisols: consequences for metal pollutant distributions. *Eur. J. Soil Sci.* 59, 925–938.
- Vingiani, S., Di Iorio, E., Colombo, C., Terribile, F., 2018. Integrated study of Red Mediterranean soils from Southern Italy. *Catena* 168, 129–140.
- Vissac, C., 2005. Study of a historical garden soil at the Grand-Pressigny site (Indre-et-Loire, France): evidence of landscape management. *J. Cult. Heritage* 6, 61–67.
- Wilkinson, T., 1988. The archaeological component of agricultural soils in the Middle East: the effects of manuring in antiquity. In: *Man-made Soils*, eds., Groenman-van Waateringe, W. and Robinson, M. Symposia of the Association for Environmental Archaeology No. 6. BAR International Series 40: Oxford. Pp. 93–114.
- WRB, I.W.G., 2015. World reference base for soil resources 2014, update 2015. *International soil classification system for naming soils and creating legends for soil maps*. *World Soil Resources Reports*, 106.
- Wouters, B., Devos, Y., Milek, K., Vrydaghs, L., Bartholomieux, B., Tys, D., Moolhuizen, C., van Asch, N., 2017. Medieval markets: A soil micromorphological

and archaeobotanical study of the urban stratigraphy of Lier (Belgium). *Quat. Int.* 460, 48–64.

Yaalon, D.H., 1997. Soils in the Mediterranean region: What makes them different? *Catena* 28, 157–169.

Yang, J.L., Zhang, G.L., 2015. Formation, characteristics and eco-environmental implications of urban soils—A review. *Soil Science and Plant Nutrition* 61 (sup1), 30–46.